ACS Infectious Diseases

pubs.acs.org/journal/aidcbc

Article

Mycobacterium tuberculosis Survival in J774A.1 Cells Is Dependent on MenJ Moonlighting Activity, Not Its Enzymatic Activity

Santosh Kumar, Jordan T. Koehn, Mercedes Gonzalez-Juarrero, Debbie C. Crans, and Dean C. Crick*

Cite This: *ACS Infect. Dis.* 2020, 6, 2661−2671

Read Online

ACCESS | Metrics & More | Article Recommendations | Supporting Information

ABSTRACT: MenJ, a flavoprotein oxidoreductase, is responsible for the saturation of the β-isoprene unit of mycobacterial menaquinone, resulting in the conversion of menaquinone with nine isoprene units (MK-9) to menaquinone with nine isoprene units where the double bond in the second unit is reduced [MK-9(II-H_2)]. The hydrogenation of MK-9 increases the efficiency of the mycobacterial electron transport system, whereas the deletion of MenJ results in decreased survival of the bacteria inside J774A.1 macrophage-like cells but is not required for growth in culture. Thus, it was suggested that MenJ may represent a contextual drug target in *M. tuberculosis*, that is, a drug target that is valid only in the context of an infected macrophage. However, it was unclear if the conversion of MK-9 to MK-9(II-H_2) or the MenJ protein itself was responsible for bacterial survival. In order to resolve this issue, a plasmid expressing folded, full-length, inactive MenJ was engineered. Primary sequence analysis data revealed that MenJ shares conserved FAD binding, NADH binding, and catalytic and C-terminal motifs with archaeal geranylgeranyl reductases. A MenJ mutant deficient in any one of these motifs is devoid of reductase activity. Therefore, point mutations of highly conserved amino acids in the conserved motifs were generated and the recombinant proteins were monitored for conformational changes by circular dichroism and oxidoreductase activity. The mutational analysis indicates that amino acids tryptophan 215 (W215) and cysteine 46 (C46) of *M. tuberculosis* MenJ, conserved in known archaeal geranylgeranyl reductases and putative menaquinone saturases, are essential to the hydrogenation of MK-9. The mutation of either C46 to serine (C46S) or W215 to leucine (W215L) in MenJ completely abolishes the catalytic activity *in vitro*, and *menJ* knockout strains of *M. tuberculosis* expressing either the C46S or W215L mutant protein are unable to convert MK-9 to MK-9(II-H_2) but survive inside the J774A.1 cells. Thus, surprisingly, the survival of *M. tuberculosis* in J774A.1 cells is dependent on the expression of MenJ rather than its oxidoreductase activity, the conversion of MK-9 to MK-9(II-H_2) as previously hypothesized. Overall, the current data suggest that MenJ is a moonlighting protein.

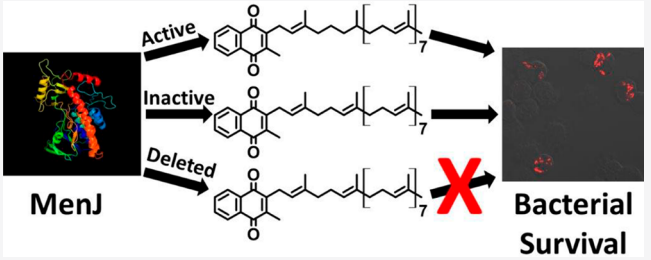

KEYWORDS: *oxidoreductase, menaquinone synthesis, menaquinone saturase, macrophage, inactivation, point mutation, circular dichroism*

Lipoquinones are lipid soluble electron carriers that transfer electrons between the essential proteinaceous components of the electron transport chain.[1,2] Bacterial respiratory lipoquinones include naphthoquinones such as menaquinone (MK) and demethylmenaquinone (DMK) and benzoquinones such as ubiquinone (UQ).[3] Both naphthoquinones and benzoquinones are characterized by isoprenoid moieties of varying chain length and degree of saturation. The structural differences in the lipoquinones (ubiquinone and menaquinone) are conserved and have been used to assist the taxonomic differentiation of prokaryotes.[3,4] *Mycobacterium* spp. use MK-9(II-H_2) (Figure 1 and Table S1), a naphthoquinone with an isoprenoid moiety consisting of nine isoprene units in the E configuration with the double bond of the isoprene unit second from the naphthoquinone ring (β-position) reduced[5−7] as the primary lipoquinone.[8,9]

MK-9(II-H_2) synthesis in mycobacteria begins with the precursor chorismate and is converted to MK through a series of reactions carried out by the MenA, B, C, D, E, F, G, and I enzymes[10−13] as shown in Figure 1. Many of these enzymes have been predicted to be essential, and several have been empirically shown to be so.[10,14−19] In *M. tuberculosis*, MenJ, a recently identified oxidoreductase, catalyzes the hydrogenation of the β-isoprene unit of MK, forming MK-9(II-H_2).[20]

The reduction of the double bond in the isoprenoid tail of MK-9 by MenJ increases the efficiency of the mycobacterial ETS system. That is, a *menJ* knockout strain of *M. tuberculosis* had reduced oxygen consumption rates and 3-fold smaller electron transport efficiency than the wild type bacteria.[20] However, the overall rate of ATP synthesis was unaltered due

Received: May 13, 2020
Published: August 31, 2020

https://dx.doi.org/10.1021/acsinfecdis.0c00312
ACS Infect. Dis. 2020, 6, 2661−2671

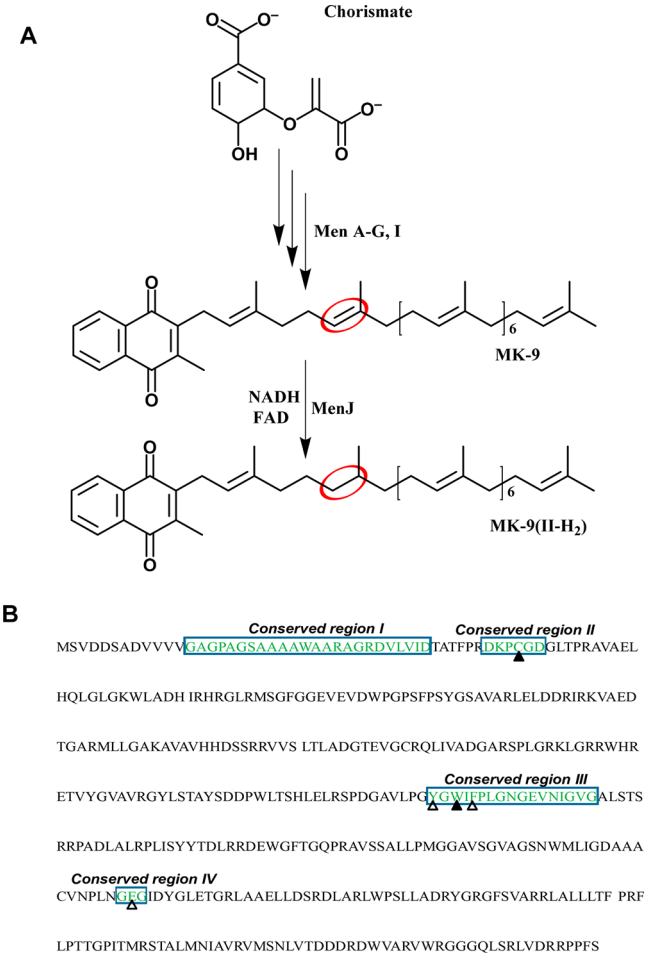

Figure 1. Menaquinone biosynthesis in mycobacteria[10,11] and the primary sequence of MenJ. (A) MenJ (*Rv0561c*) catalyzes the production of MK-9(II-H_2) from MK-9.[20,33] The bond hydrogenated by MenJ is circled in red. (B) Multiple sequence alignments identified motifs sharing high amino acid sequence homology between archaeal GGRs and mycobacterial MenJ. Four conserved motifs, boxed and indicated in green, were selected for deletion mutagenesis. Triangles indicate the amino acid residues chosen for point mutagenesis. Mutations of amino acids indicated by the closed triangles cause a complete loss of oxidoreductase activity. Mutations of amino acids indicated by the open triangles cause a reduction in oxidoreductase activity.

to compensation by increased levels of total MK production. The disruption of MenJ in both *M. tuberculosis* and *M. smegmatis* results in strains that show no growth phenotypes in rich medium under aerobic or hypoxic conditions. Interestingly, however, a *menJ* knockout strain of *M. tuberculosis* showed highly attenuated survival in mouse macrophage-like J774A.1 cells. Complementation of the knockout strain with recombinant MenJ was able to restore the intracellular survival.[20] These observations led to the hypothesis that the saturation of the β-isoprene unit of mycobacterial MK by MenJ may represent a conditional drug target in a testable system.[20] However, in the reported *menJ* knockout mutation, a large portion of the wild-type open reading frame is replaced by an in-frame kanamycin cassette.[20] Thus, the mutant strain of bacteria was deficient in both MK-9(II-H_2), the product of MenJ, and MenJ itself, which created the possibility, however unlikely, that the observed survival phenotype is due to the deficiency of the MenJ protein rather than its MK saturase activity. Thus, the experiments described here were designed to clarify this issue and required the engineering of a mutant MenJ protein that was full length, folded correctly, and inactive.

On the basis of amino acid sequence similarity, MenJ is classified as a member of the geranylgeranyl reductase (GGR) family of enzymes,[20] which also has member proteins expressed in Archaea, bacteria, and plants.[21−23] The GGR family of enzymes typically consists of multifunctional, hydrogenating multiple isoprene units of bacteriochlorophyll, chlorophyll, tocopherol, phylloquinone, or archaeal phospholipids in a stepwise fashion.[21−23] Protein primary sequence alignments demonstrate that MenJ is highly conserved throughout the mycobacterial species, for example *Mycobacterium smegmatis* expresses a homologue, MSMEG 1132, with 74% identity. In addition, the enzyme has 24−25% amino acid identity to GGRs identified in *Thermoplasma acidophilum* and *Sulfolobus acidocaldarius*, organisms from which the GGRs have been purified and crystallized.[24,25] The crystal structures and mutagenesis of these proteins revealed four conserved regions of primary sequence associated with nucleotide and substrate binding[24,25] (Figure S1).

The first conserved amino acid motif [GxGxxGx17-18(D/E)] likely interacts with FAD, stabilizing it;[26] the motif is also found in members of the *p*-hydroxybenzoate hydroxylase (PHBH) family of flavoenzymes.[27] The second conserved motif, composed of residues PVRCGE and DKPCDG in *T. acidophilum* and *S. acidocalderius*, respectively, also interacts with FAD.[24,25] The conservation of the cysteine residue in this motif is interesting because it directly interacts with the isoalloxazine of FAD.[24,25] Mutation analysis of the *S. acidocaldarius* enzyme indicated that this residue is vital to protein activity and is likely involved in catalysis.[25] The third conserved motif (YxWxFPx7-8GxG) holds the ligand in place for reduction.[24,25] The fourth and final motif (G(G/E)G) is also located near the isoalloxazine ring, and the third amino acid (G) is generally conserved in related FAD binding proteins.[25] More recent analysis of demonstrably active GGRs indicates that while overall sequence identities are low, the predicted FAD binding and catalytic motifs are conserved,[24,25,28−32] providing a convenient starting point for the experiments reported here.

RESULTS

Conserved Amino Acid Motifs in MenJ Orthologs. Multiple sequence alignment analysis of the primary amino acid sequences of MenJ from *M. tuberculosis* and *M. smegmatis* with the sequences of eight GGRs,[28] seven archaeal and one bacterial, of demonstrated activity detected all four of the conserved domains identified in the archaeal GGRs from *T. acidophilum* and *S. acidocalderius* (Figures 1 and S1). On the basis of the sequence alignment results, in-frame PCR-based motif deletion mutants of these conserved regions in mycobacterial MenJ (named ΔRegion I, ΔRegion II, ΔRegion III, and ΔRegion IV) were constructed. The mutations were confirmed by DNA sequencing and subsequently cloned in the pMyNT expression vector. The resulting constructs, including an empty vector, were used to transform *M. smegmatis* Δ*MSMEG1132*. The resulting recombinant strains were grown in 7H9 media, and the cultures were induced with 0.2% (w/v) acetamide for protein expression when the OD reached 0.5 and incubated for another 24−36 h. Cells were then harvested and lipids were extracted as previously

https://dx.doi.org/10.1021/acsinfecdis.0c00312
ACS Infect. Dis. 2020, 6, 2661−2671

described.[18,20] Levels of protein expression were judged to be similar on the basis of SDS-PAGE analysis and Western blot analysis of equal masses of protein. MK was analyzed by mass spectrometry coupled with HPLC. The identification of MK was based on the retention time and observation of the protonated molecular ion, $[M + H]^+$. The calculated monoisotopic mass of MK-9 is 784.6158 Da, and the expected m/z value for $[M + H]^+$ is 785.6362 Da. If one isoprene unit is reduced, forming MK-9(II-H_2), then the calculated monoisotopic mass is 786.6315 Da and expected $[M + H]^+$ is 787.6368 Da. As shown in Figure S2, only the lipids isolated from *M. smegmatis* Δ*MSMEG1132* transformed with wild-type MenJ exhibited a strong feature with an observed m/z of 787.6 at a retention time of 28.5 min, confirming the presence of MK-9(II-H_2) as previously reported.[20] Lipids isolated from *M. smegmatis* Δ*MSMEG1132* transformed with an empty vector or the motif deletion mutants (ΔRegion I, ΔRegion II, ΔRegion III, and ΔRegion IV) of MenJ all exhibited a peak with an observed m/z of 785.6 and a retention time of 24.5 min (Figure S2). The observed feature at the m/z 787.6 peak coincident with m/z 785.6 at a retention of 24.5 min represents an isotopic peak. Thus, the *M. smegmatis menJ* knockout strain (*M. smegmatis* Δ*MSMEG1132*) synthesized MK-9 as previously reported,[20,33] and the deletion of any of the conserved motifs abolishes enzymatic activity.

LC−MS Analysis of Lipids Isolated from *M. tuberculosis* H37Δ*Rv0561c* Transformed with Wild Type MenJ and MenJ with Point Mutations. The data obtained from *M. smegmatis* Δ*MSMEG1132* transformed with an empty vector or the motif deletion mutants (above) suggested that there could be single amino acids within the motifs which could potentially be mutated to produce inactive protein that is full length and folds properly. Therefore, site-directed mutagenesis was used to construct genes that would express proteins with single point mutations (C46S, Y213L, W215L, F217L, and E301G) in the conserved regions of the *M. tuberculosis* protein. A *menJ* knockout strain (H37Δ*Rv0561c*) of *M. tuberculosis* was transformed with vector-expressing protein from wild type *menJ* or the mutated versions of *menJ*. Lipids were extracted from the bacterial strains and analyzed by LC−MS as described above. The lipids isolated from *M. tuberculosis* H37Δ*Rv0561c* were transformed with pMyNT (empty vector) and contained a peak with an observed m/z of 785.6 and a retention time of 12.2 min (Figure 2). The lipids isolated from *M. tuberculosis* H37Δ*Rv0561c* transformed with wild type MenJ (complemented) contained a strong peak of m/z at 787.6 and a retention time of 13.8 min (Figure 2), confirming the presence of MK-9(II-H_2) as reported earlier.[20] Moreover, lipids isolated from bacteria expressing the W215L and C46S mutations of MenJ contained a strong peak with an observed m/z of 785.6 and a retention time of 12.2 min (representing MK-9, Figure 3). The observed feature at the m/z 787.6 peak coincident with m/z 785.6 at a retention of 12.2 min represents an isotopic peak. However, lipids isolated from bacteria expressing the Y213L, F217L, and E301G mutations all have two features at m/z 787.6: one representing an isotopic peak coincident with the m/z 785.6 feature and a new feature at 787.6 m/z representing MK-9(II-H_2).

The level of protein expression was also monitored in all bacterial strains. After lipid extraction, the remaining cell pellets were solubilized and the protein content was estimated. Equal amounts of protein from each strain were analyzed by SDS-PAGE, followed by immunoblotting (Figure 4). The data

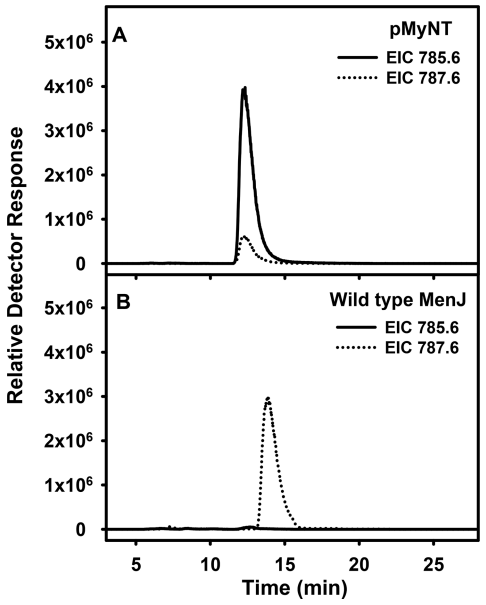

Figure 2. Extracted ion chromatograms of LC−MS analysis of the lipids isolated from *M. tuberculosis* H37Δ*Rv0561c* transformed with an empty vector or a vector expressing wild type MenJ (*Rv0561c*). Extracted ion chromatograms (EIC) were generated from total ion chromatograms (TIC) by extracting the collected data for ions with $[M + H]^+$ at m/z 785.6 ± 0.5 or m/z 787.6 ± 0.5 for MK-9 or MK-9(II-H_2), respectively. (A) *M. tuberculosis* H37Δ*Rv0561c* transformed with an empty vector (pMyNT). (B) *M. tuberculosis* H37Δ*Rv0561c* transformed with a vector containing *menJ*.

shows that the point mutations introduced do not change the expression of the protein.

In addition, a similar set of experiments were performed using surrogate host *M. smegmatis* Δ*MSMEG1132*. All results were similar to those seen using *M. tuberculosis* H37Δ*Rv0561c* as the expression host (Figures S3 and S4), with the only obvious difference being that the lipids isolated from the Y213L, F217L, and G301E show quantitatively greater amounts of MK-9(II-H_2) when expressed in the surrogate.

Effect of Point Mutations on MenJ Oxidoreductase Activity. Wild type MenJ and MenJ containing point mutations C46S, Y213L, W215L, F217L, and E301G were expressed in *M. smegmatis* and purified to near homogeneity by immobilized metal affinity chromatography. These proteins were monitored for changes in secondary and tertiary structure by circular dichroism[34] spectroscopy. This analysis did not suggest that the introduction of the point mutations caused a gross alteration in the folding pattern of any of the proteins (Figure S5). The impact of the point mutations on the oxidoreductase activity of the proteins was also evaluated. The oxidoreductase activity was reduced to undetectable levels in the C46S and W215L mutants as expected from the lipid analysis described above. When assayed using NADH as the donor and UQ-1, the Y213L, F217L, and E301G mutants exhibited similar or slightly less activity than did the wild type at the same enzyme concentration.

Kinetic Properties of Wild Type MenJ and the Y213L, F217L, and E301G Mutants. The oxidoreductase activity of wild type MenJ and the mutant proteins were measured by monitoring the reduction of two lipoquinones, UQ-1 and MK-1 acceptor molecules, under the conditions described in the figure and table legends. Representative Michaelis−Menten

https://dx.doi.org/10.1021/acsinfecdis.0c00312
ACS Infect. Dis. 2020, 6, 2661−2671

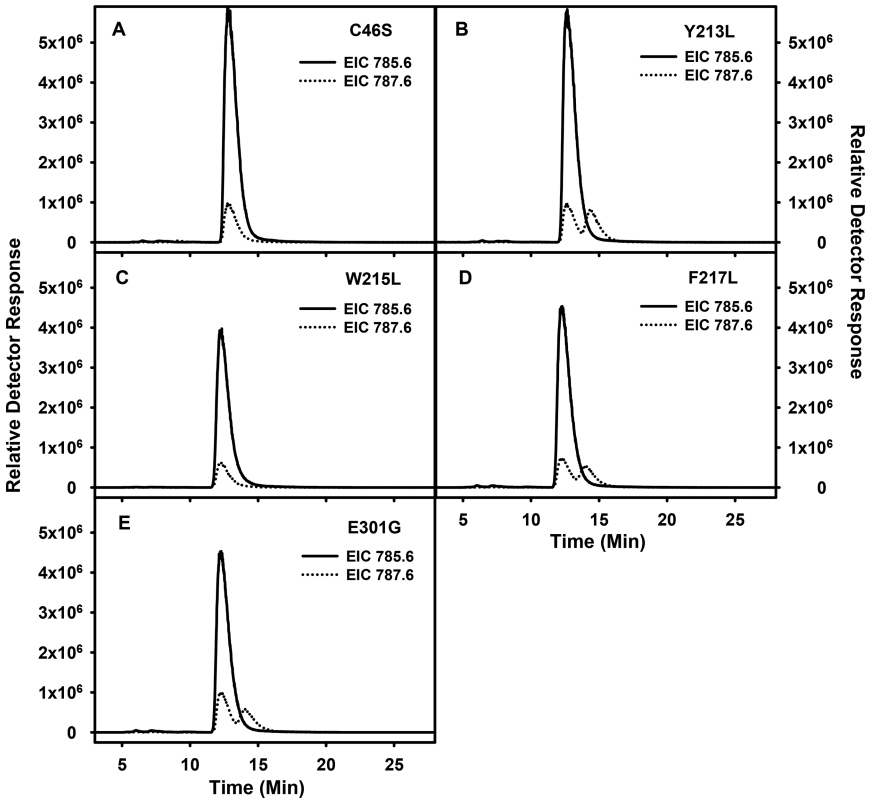

Figure 3. Extracted ion chromatograms of LC−MS analysis of the lipids isolated from *M. tuberculosis* H37Δ*Rv0561c* transformed with plasmids encoding MenJ containing point mutation C46S, Y213L, W215L, F217L, or E301G. Extracted ion chromatograms (EICs) were generated from total ion chromatograms (TICs) by extracting collected data for ions with $[M + H]^+$ at m/z 785.6 ± 0.5 or m/z 787.6 ± 0.5 for MK-9 or MK-9(II-H_2), respectively. *M. tuberculosis* H37Δ*Rv0561c* was transformed with (A) *pMyNT-Rv0561c(C46S)*, (B) *pMyNT-Rv0561c(Y213L)*, (C) *pMyNT-Rv0561c(E301G)*, (D) *pMyNT-Rv0561c(W215L)* and (E) *pMyNT-Rv0561c(F217L)*.

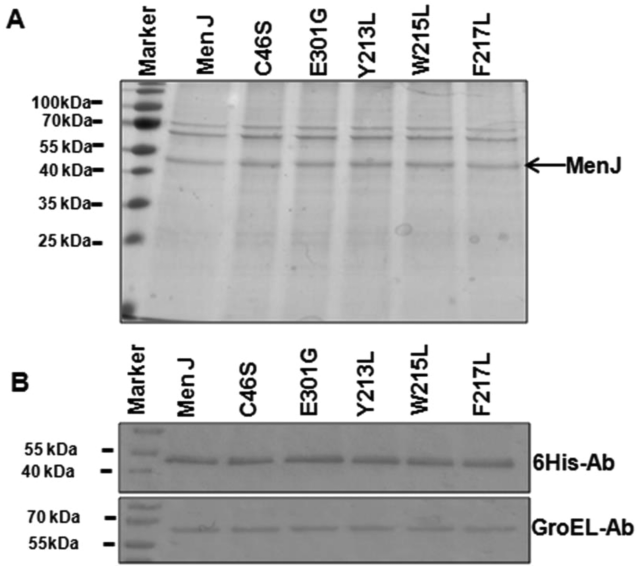

Figure 4. Expression of MenJ in various strains of *M. tuberculosis*: *M. tuberculosis* H37Δ*Rv0561c* was transformed with plasmids encoding MenJ or MenJ containing point mutation C46S, Y213L, W215L, F217L, or E301G. Cells were harvested after induction with acetamide and homogenized, and equal amounts of whole cell lysate (20 μg) containing recombinant protein were loaded into each lane and subjected to analysis by SDS-PAGE stained with AcquaStain protein stain (A) and Western blot using the 6X anti-His antibody GroEL antibody CS-44 as a loading control (B).

curves for wild type and mutated MenJ are shown in Figures 5 and S6, respectively. The calculated kinetic parameters are shown in Table 1.

The K_m value of wild type MenJ for MK-1, a naphthoquinone, in the presence of saturating levels of NADH is 30 ± 2 μM, whereas the K_m for UQ-1, a benzoquinone, is 50 ± 2 μM (Table 1). The V_{max} and consequently the k_{cat} values calculated for MK-1 are ∼3-fold lower than those for UQ-1. In comparing the wild type MenJ to the mutant versions of MenJ, clear trends are seen. In the case of steady-state kinetics using UQ-1 as the acceptor substrate, the three mutant proteins, Y213L, F217L, and E301G, all show significantly reduced K_m and k_{cat} values relative to the wild type (Table 1). This is also reflected in the calculated k_{cat}/K_m values. However, when MK-1 is utilized as the acceptor substrate, a significant reduction of K_m is seen in the Y213L mutant (Table 1), with no significant changes for the F217L and E301G mutants relative to the wild type. In addition, the V_{max} and k_{cat} values for all three mutant proteins were unchanged relative to the wild type. K_m^{NADH} was unchanged in any of the proteins tested, and k_{cat}^{NADH} was similar in all proteins except Y213L, where it was significantly reduced by 2-fold (Table 1).

MenJ Is Essential to the Survival of Bacilli Inside the Macrophage. J774A.1 macrophage-like cells were infected with *M. tuberculosis* H37Rv, *M. tuberculosis* H37Δ*Rv0561c*/pMyNT, *M. tuberculosis* H37Δ*Rv0561c/menj*, *M. tuberculosis* H37Δ*Rv0561c/menj(C46S)*, *M. tuberculosis* H37Δ*Rv0561c/menj(W215L)*, and *M. tuberculosis* H37Δ*Rv0561c/menj-*

https://dx.doi.org/10.1021/acsinfecdis.0c00312
ACS Infect. Dis. 2020, 6, 2661−2671

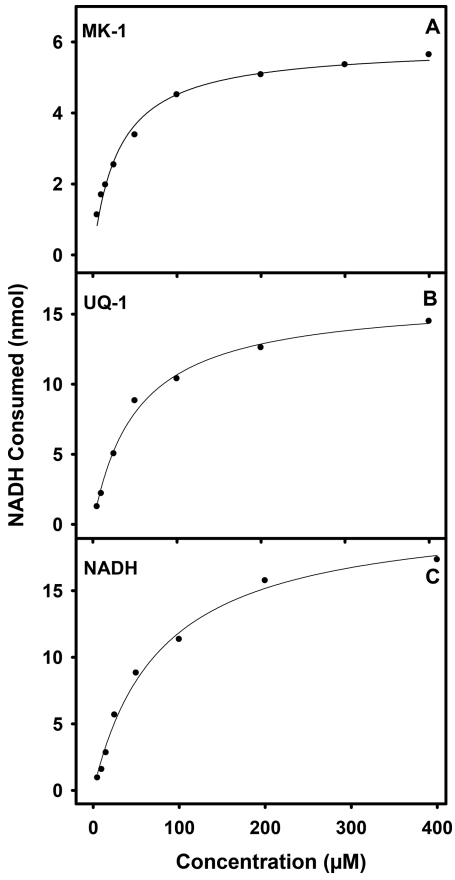

Figure 5. Representative Michaelis–Menten curves. Panels A and B show the effects of MK-1 or UQ-1 concentration, respectively, on wild type MenJ activity at 150 μM NADH. Panel C shows the effect of NADH concentration at 200 μM UQ-1. Assays also contained 500 ng of MenJ and 0.1 M McIlvaine's buffer (pH 7.0) in a final volume of 200 μL, and they were incubated at 37 °C for 30 min. Calculated kinetic parameters can be found in Table 1.

(Y213L) at an MOI of 5 bacilli/J774A.1 cell in order to determine if MenJ or MK-9(II-H_2) is required for bacteria survival. After 2 h of incubation, the nonadherent bacteria were removed by extensive washing, and the infected cells were fixed and stained. The association of bacteria with macrophage cells was determined by confocal fluorescence microscopy. Microscopic examination indicated that the acid-fast bacilli were exclusively associated with eukaryotic cells (Figure 6).

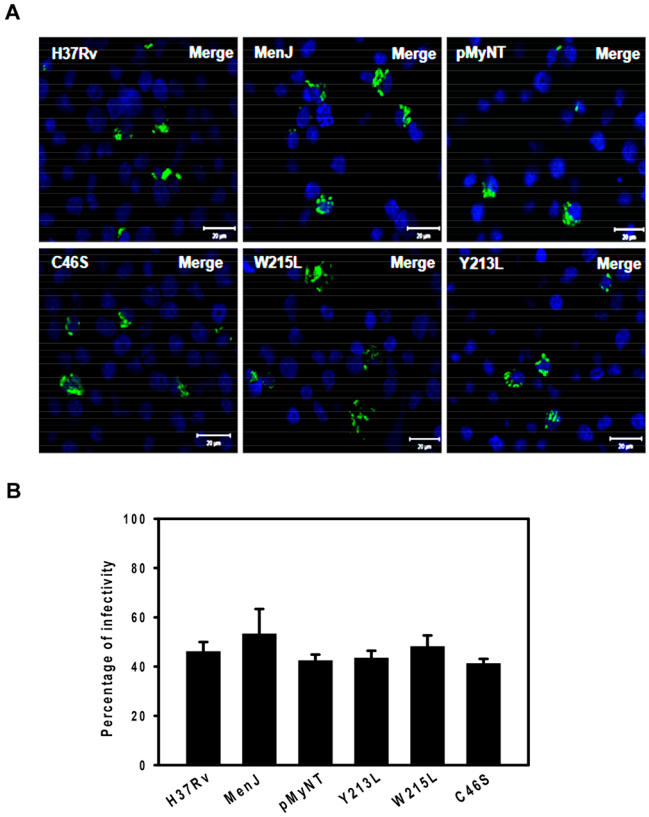

Figure 6. Infection of J774A.1 cells with various strains of *M. tuberculosis*. (A) Fluorescent images of J774A.1 cells infected with *M. tuberculosis* H37Rv (wild type) or *M. tuberculosis* H37Δ*Rv0561c* transformed with plasmids encoding MenJ (*Rv0561c*) or MenJ containing point mutation C46S, Y213L, or W215L at an MOI of 5:1 (bacteria/J774A.1 cell). Cells were then incubated at 37 °C under 5% CO_2 for 2 h and exhaustively washed. Infected cells were fixed and stained with acid-fast SYBR Gold[17] and counterstained with DAPI (blue). Images were captured at 63× magnification in an LSM 510 META confocal microscope. The scale bar is 20 μm. (B) Percentage infectivity determined by counting four randomly selected fields of cells infected with each bacterial strain.

Table 1. Kinetic Parameters of MenJ and Mutant Proteins[a]

	varied substrate					
	NADH		MK-1		UQ-1	
enzymes	K_m (μM)	k_{cat} (S^{-1})	K_m (μM)	k_{cat} (S^{-1})	K_m (μM)	k_{cat} (S^{-1})
Rv0561c	76 ± 6.8[a]	1.01 ± 0.04[a]	30 ± 2.0[a]	0.27 ± 0.03[a]	50 ± 2.0[a]	0.94 ± 0.14[a]
C46S	nd	nd	nd	nd	nd	nd
Y213L	72 ± 6.0[a]	0.50 ± 0.01[b]	13 ± 1.9[b]	0.26 ± 0.01[a]	17 ± 6.3[c]	0.23 ± 0.01[c]
W215L	nd	nd	nd	nd	nd	nd
F217L	76 ± 3.4[a]	1.06 ± 0.03[a]	20 ± 3.0[a]	0.23 ± 0.01[a]	35 ± 9.6[b]	0.49 ± 0.11[b]
E301G	72 ± 3.8[a]	1.05 ± 0.02[a]	25 ± 3.7[a]	0.26 ± 0.01[a]	30 ± 7.1[b,c]	0.35 ± 0.02[b,c]

[a]Steady-state kinetic parameters were measured in 0.1 M McIlvaine's buffer (pH 7.0) in a final volume of 200 μL and were incubated at 37 °C for 30 min. The reaction mixture also contained 500 ng of MenJ and varying concentrations of MK-1, UQ-1, or NADH. Kinetics parameters for MK-1 were determined in the presence of 0.5% Tween 80 and saturating levels of NADH. The reductase activity was measured by monitoring the NADH consumption spectrophotometrically by following the decrease in absorbance at 340 nm (UQ-1) and 360 nm (MK-1). K_m and k_{cat} values were calculated using GraFit-5 software. Values indicated are the averages of three experiments ± the standard deviation. Representative Michaelis–Menten curves are presented in Figure 5 and Figure S5. Values in each column with the same superscript are not significantly different. (See the Supporting Information for statistical analysis.) nd: enzyme activity not detected.

https://dx.doi.org/10.1021/acsinfecdis.0c00312
ACS Infect. Dis. 2020, 6, 2661–2671

Individual infected macrophage-like cells contained variable numbers of bacilli ranging from one to several. The infection ratio, the number of J774A.1 cells/number of bacilli, was ~42% and was similar for all strains of *M. tuberculosis* used (Figure 6).

J774A.1 cells infected for 0, 1, 2, 3, and 4 days were homogenized, and the resulting homogenates were plated on 7H11 agar with and without hygromycin B to determine the numbers of viable colony-forming units (CFU, Figure 7). The

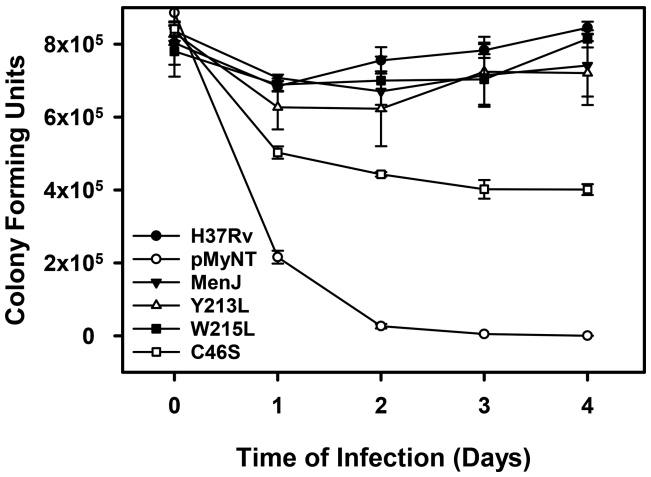

Figure 7. Survival of *M. tuberculosis* strains in J774A.1 cells. J774A.1 cells were infected with *M. tuberculosis* H37Rv (wild type) or *M. tuberculosis* H37Δ*Rv0561c* transformed with plasmids encoding MenJ (*Rv0561c*) or MenJ containing point mutation C46S, Y213L, or W215L. The *M. tuberculosis* burden was determined in homogenates from cells infected for 0, 1, 2, 3, and 4 days. Serial dilutions of homogenates were plated on 7H11 agar plates containing hygromycin B (except for homogenates containing *M. tuberculosis* H37Rv) to determine the number of colony-forming units. Values shown are averages of three independent experiments, and error bars indicate the standard deviation of the mean. See the Supporting Information for statistical and regression analysis.

CFU counts at each time point were subjected to ANOVA and pairwise multiple comparisons (Supporting Information). At 0 days of infection, there was no statistical difference in the numbers of CFU recovered from each strain of *M. tuberculosis*, confirming the results of the confocal microscopy. However, the survival of *M. tuberculosis* H37Δ*Rv0561c*/pMyNT, devoid of MenJ, rapidly decreased over time, and the CFU counts for this strain were significantly lower than for the other strains at all other time points. All bacterial strains expressing MenJ, whether active, partially active, or inactive, survived along with wild type *M. tuberculosis* (H37Rv) in the macrophage-like cells except the strain expressing the C46S mutant, which had ~2-fold reduced viability that was statistically significant by the second day of infection. However, the H37Δ*Rv0561c*/*menj(C46S)* strain survived significantly better than the H37Δ*Rv0561c*/pMyNT strain at all time points from 1 day of incubation on. This trend is clearly shown in Figure S7, where regression analysis of a semilog plot of the same data is presented.

DISCUSSION

Deletion of Conserved Motifs Causes Complete Loss of Oxidoreductase Activity. Multiple sequence alignments detected four motifs that share amino acid sequence homology between archaeal GGRs and mycobacterial MenJ. The deletion of these motifs in MenJ did not affect the expression of the recombinant enzymes relative to the expression of recombinant wild type enzyme. However, MS analysis of lipids extracted from bacterial strains expressing the mutated proteins indicated that these modified proteins had completely lost their oxidoreductase activity and were unable to synthesize MK-9(II-H_2). Thus, each of the motifs is essential to oxidoreductase activity, likely due to interactions with the FAD cofactor and the substrate as previously determined in the archaeal enzymes.[24,25]

Effects of Point Mutations (C46S, Y213L, W215L, F217L, and E301G) in MenJ. The overall goal of the experiments described here was to determine the relative importance of MenJ or its product to survival in macrophages. This objective required the expression of a mutant MenJ protein that was full length, folded correctly, and inactive. Therefore, genes were engineered to express MenJ with point mutations in conserved regions that had previously been identified as potentially being involved in oxidoreductase activity.[24,25,28] Wild-type MenJ and mutated MenJ were successfully expressed in knockout strains of *M. tuberculosis* (*M. tuberculosis* H37Δ*Rv0561c*) and *M. smegmatis* (*M. smegmatis* Δ*MSMEG1132*). The isolated lipids from these recombinant wild type MenJ and MenJ mutants were subjected to MS analysis, which indicated that *M. tuberculosis* H37Δ*Rv0561c* transformed with pMyNT-containing genes for MenJ C46S or W215L did not synthesize detectable amounts of MK-9(II-H_2). Moreover, MenJ containing mutations Y213L, F217L, and G301E did synthesize MK-9(II-H_2) but functioned at reduced rates relative to the bacilli transformed with the vector expressing wild type MenJ. These results were consistent when the proteins were expressed in either *M. tuberculosis* or the surrogate host, *M. smegmatis*.

Importantly, the introduction of the point mutations did not appreciably affect either the levels of expression or the protein folding in either host species. However, when the impact of the mutations on the oxidoreductase activity of purified, recombinant protein was evaluated, the oxidoreductase activity was undetectable in the C46S and W215L mutants, an observation that is consistent with the MS data. The Y213L, F217L, and E301G mutants exhibited similar or slightly less activity than did the wild type at the same concentration in the assays.

The kinetic properties of the wild type and mutated protein were also compared using steady-state kinetics, NADH as the donor, UQ-1 or MK-1 as the acceptor substrate, and Michaelis–Menten assumptions. Initially, commercially available MK-4 and MK-9 were used as potential acceptor substrates; however, no enzyme activity could be detected using these compounds. This may be due to a lack of solubility in aqueous solutions (MK-4 and MK-9 have calculated log *P* values of 11 and 21, respectively). Fortunately, chemically synthesized MK-1 with a calculated log *P* value of 4.8 and the more soluble, commercially available UQ-1 could be utilized as lipoquinone substrates as previously published.[33]

With respect to the wild type enzyme, K_m^{NADH}, K_m^{MK-1}, and K_m^{UQ-1} were found to be 76 ± 6.8, 30 ± 2.0, and 50 ± 2.0 μM, respectively (Table 1). These values are consistent with the previously published values and confirm that the enzyme is not specific for either the naphthyl or the benzyl ring,[33] although K_m^{MK-1} is statistically significantly lower than K_m^{UQ-1}. In addition, k_{cat}^{MK-1} was 3-fold lower than k_{cat}^{UQ-1}. This difference

https://dx.doi.org/10.1021/acsinfecdis.0c00312
ACS Infect. Dis. 2020, 6, 2661−2671

was also statistically significant. The differences in affinity and rates of substrate turnover may be due to the structural differences in these acceptors, the difference in solubility, or, more likely, a combination of the two. It should be noted that neither of these substrates is an exact analog of the natural substrate (MK-9) because the short isoprenyl chain on each does not have the β-isoprene double bond that is reduced *in vivo*.[20,33]

The K_m^{NADH} value of the Y213L, F217L, and E301G mutants was unchanged relative to that of the wild type enzyme, whereas the k_{cat}^{NADH} value was significantly reduced in the Y213L mutant and unchanged in the F217L and E301G mutants. K_m^{MK-1} was significantly reduced in the Y213L mutant but not in the F217L or E301G mutant. The k_{cat}^{MK-1} values determined for all three mutants were similar to the wild type values. K_m^{UQ-1} and k_{cat}^{UQ-1} values were reduced in Y213L, F217L, and E301G mutants relative to those in the wild type enzyme. Thus, these three mutations do not seem to affect the affinity for NADH but increase the affinity for and reduce the turnover of UQ-1. However, they have little effect on the turnover of MK-1 and affect only the affinity, which is somewhat increased in the case of Y213L.

Taken together, the data obtained from the C46S, Y213L, W215L, F217L, and E301G point mutations are consistent with earlier work with GGRs that suggested that the motifs containing C46, Y213, W215, F217, and E301 in *M. tuberculosis* MenJ are associated with the active site and that the latter four residues are likely involved in substrate interactions.[24,28] However, in MenJ, C46 and W215 are absolutely required for oxidoreductase activity. These mutants had undetectable activity *in vivo* and *in vitro*, whereas the mutation of the corresponding residues in the GGR from *S. acidocalderius* resulted only in an uncharacterized decrease in activity.[25]

MenJ but Not Its Oxidoreductase Activity Is Required for the Survival of Bacilli inside the Macrophage. J774A.1 macrophage-like cells were infected with *M. tuberculosis* H37Rv, *M. tuberculosis* H37Δ*Rv0561c/pMyNT*, *M. tuberculosis* H37Δ*Rv0561c/menj*, *M. tuberculosis* H37Δ*Rv0561c/menj(C46S)*, *M. tuberculosis* H37Δ*Rv0561c/menj(W215L)*, and *M. tuberculosis* H37Δ*Rv0561c/menj-(Y213L)* at a MOI 5 bacilli/J774A.1 cell in order to determine if MenJ or MK-9(II-H_2) is required for bacterial survival. As noted above, all proteins are expressed at similar levels from pMyNT in *M. tuberculosis*. *M. tuberculosis* H37Rv and strains of *M. tuberculosis* transformed with an empty vector or a vector expressing recombinant protein all infected the J774A.1 cells equally. That is, the infection ratio was similar for all strains of *M. tuberculosis* used. Thus, expression or the lack of expression of MenJ has no effect on bacterial infectivity. However, the expression of MenJ significantly affected bacterial survival in the macrophage-like cells. The survival of *M. tuberculosis* H37Δ*Rv0561c/pMyNT*, devoid of MenJ, rapidly decreased over time, as was previously reported.[20] Surprisingly, all bacterial strains expressing MenJ, whether demonstrating full oxidoreductase activity, partial activity, or no activity, survived in the J774A.1 cells. The only variation was shown by the *M. tuberculosis* H37Δ*Rv0561c/menj(C46S)* strain, which had a statistically significant 2-fold reduction in survival. The basis of this reduced survival is not immediately clear. The MenJ C46S mutant protein has no observable oxidoreductase activity but neither does the MenJ W215L mutant, and the *M. tuberculosis* H37Δ*Rv0561c/menj(W215L)* strain survives like the wild type. Thus, it is concluded that the expression of the protein, MenJ, rather than its catalytic activity or the formation of MK-9(II-H_2) is required for survival in the J774A.1 cells.

It was previously hypothesized that the oxidoreductase activity of MenJ was responsible for the bacterial survival in the eukaryotic cells.[20] On the basis of the observation that the deletion of MenJ resulted in a loss of electron transport efficiency and the ability to survive in the macrophage, conventional wisdom dictated that the structural changes in the lipoquinone induced by the reduction of the double bond to form MK-9(II-H_2) could be a virulence factor. However, the current data indicates that this is not the case. Furthermore, it is now clear that the oxidoreductase activity of MenJ does not constitute a conditional drug target as suggested.

The mechanism by which MenJ promotes survival in J774A.1 cells is currently unclear. It is possible, although unlikely, that the enzyme has a second, undiscovered catalytic activity, but conserved domain searches do not provide any insight in this regard. Thus, MenJ appears to meet the canonical definition of a "moonlighting" protein, that is, a protein where one polypeptide chain exhibits multiple physiologically relevant biochemical or biophysical functions that are not due to gene fusions or multiple proteolytic fragments.[35] Significant numbers of moonlighting proteins have been identified in bacteria including mycobacteria; currently there are 11 *M. tuberculosis* proteins listed in the MoonProt database. Moonlighting proteins are often identified in pathogens and associated with bacterial virulence, although the prevalence in pathogens is likely a consequence of the extra attention paid to these organisms. Proteins shown to have moonlighting activity in bacterial virulence include metabolic enzymes of the glycolytic and other pathways such as the glyoxylate cycle, molecular chaperones, and protein-folding catalysts.[36] These cytosolic proteins are often secreted, surface-associated, and function in bacterial adhesion, signaling, and leukocyte activity modulation.[36−39] Since MenJ is a membrane-associated enzyme and does not seem to be associated with adhesion to or the invasion of host cells, it does not appear to fall into this category of moonlighting proteins. However, there are other activity combinations that have been observed less often.[39] For example, cytidine 5′-triphosphate (CTP) synthase (CtpS), in *Caulobacter crescentus*, is an essential protein that functions metabolically and plays a cytosketetal role in cell shape determination.[40] Interestingly, a NADPH:quinone oxidoreductase was among the first moonlighting proteins identified; this enzyme moonlights as the ζ-crystallin of the guinea pig lens.[41] Thus, it is also possible that MenJ acts as a structural protein, which is essential for bacterial survival in macrophage-like cells. Since the identification of moonlighting functions is difficult and often serendipitous, efforts to determine of the precise moonlighting function of MenJ are ongoing.

However, *menJ* is, as previously predicted, essential to *M. tuberculosis* survival in murine macrophages.[42] What is now clear is that the expression of the MenJ protein is, in fact, required for *M. tuberculosis* survival in the macrophage and that survival is unrelated to its oxidoreductase activity. It appears likely that MenJ is directly involved in host−pathogen interactions or plays a structural role, which may alter virulence.

https://dx.doi.org/10.1021/acsinfecdis.0c00312
ACS Infect. Dis. 2020, 6, 2661−2671

METHODS

Materials. All of the bacterial strains and plasmids used in this study are described in Table S2. High Fidelity Taq DNA polymerase was from Roche Diagnostics, and BCA protein assay kits were purchased from Thermo Scientific Pierce. Quick-change XL site-directed mutagenesis kits were purchased from Agilent Technologies. The oligonucleotide primers listed in Table S3 were synthesized from Integrated DNA Technologies. Plasmid mini-prep, PCR purification kits, Sybr Gold stain, and DAPI (4′,6-diamidino-2-phenylindole) were acquired from Thermo Fisher Scientific. Prolong Gold AntiFade Reagent was from Invitrogen. Protein staining reagent (AcquaStain) was from Bulldog Bio. Tissue culture flasks and cell scrapers were obtained from Corning and BD Falcon, respectively. Hygromycin B was from Calbiochem. Bacterial media and growth supplements (7H9, 7H10, OADC, and LB) were from BD Difco. Vitamin K2 (MK-4), UQ-1, NADH, FAD, sodium cholate, sodium deoxycholate, goat antimouse IgG alkaline phosphatase conjugate secondary antibody, BCIP/NBT tablets, acetamide, complete protease inhibitor cocktail, Ni-NTA beads, and trypan blue were purchased from Sigma-Aldrich. The 6X-His tag antibody was from Invitrogen, and the anti-GroEL antibody (CS-44) was from BEI Resources. MK-1 was synthesized as previously reported.[33,43]

Subcloning of *menJ* (*Rv0561c*) in the pMyNT Expression Vector. The *Rv0561c* gene was subcloned into pMyNT, an *E. coli*/mycobacteria shuttle expression vector[44] between NcoI and *Hin*dIII restriction sites. The pMyNT-*Rv0561c* construct was used to transform *M. smegmatis* Δ*MSMEG1132* bacteria. A single, well-isolated colony was used to inoculate 10 mL of 7H9Middlebrook medium, supplemented with 0.2% (v/v) glycerol, 10% ADC, 0.05% Tween-80, and 50 μg/mL hygromycin B and was incubated at 37 °C for 36 h. The growth culture was used to inoculate 1000 mL of supplemented Middlebrook 7H9 medium, which was incubated at 37 °C until the OD_{600} reached 0.5 to 0.7. Protein expression was then induced by the addition of 0.2% (w/v) acetamide before incubation for another 24−36 h at 37 °C[44] prior to harvest. Harvested cells were suspended in HEPES/phosphate buffer (50 mM HEPES/50 mM potassium phosphate, pH 7.0, containing 1 mM phenylmethylsulfonyl fluoride) and stored at −80 °C.

Purification of Recombinant MenJ from *M. smegmatis* Δ*MSMEG1132*. The harvested bacteria were broken by sonication. Sodium cholate and sodium deoxycholate (1% each) were added to the suspension and stirred on ice for 1 h.[45] The detergent-solubilized homogenate was obtained by centrifugation at 27 000*g* for 30 min at 4 °C. The solubilized fraction was then incubated at 4 °C with Ni-NTA beads (Sigma). Bound protein was eluted with HEPES/phosphate buffer containing 0.25% sodium cholate and 250 mM imidazole at pH 7.4. Eluted protein was further purified using a PD-10 column and was concentrated by ultrafiltration. The purity of the protein was assessed with 12% SDS-PAGE. The concentration of protein was determined using a BCA protein assay kit, glycerol was added to 10% (v/v), and aliquots of protein were stored at −80 °C.

Measurement of MenJ UQ-1 Oxidoreductase Activity. For purified wild type MenJ and the cognate mutants, oxidoreductase activity was measured as described earlier.[33] Briefly, the standard reaction buffer contained 150 μM NADH, 200 μM coenzyme Q-1 (UQ-1) as the substrate, and 0.5 μg of purified MenJ in 0.1 M Mcllvaine's buffer (pH 7.0). The MenJ reductase activity was measured by monitoring the NADH consumption spectrophotometrically by following the decrease in absorbance at 340 nm in a 200 μL reaction mixture at 37 °C.[46]

Measurement of MenJ MK-1 Oxidoreductase Activity. MK-1 was solubilized in 20% Tween-80, which was diluted to a final concentration of 0.5% in the assay mixtures described above, and the activity was monitored by the change in absorbance at 360 nm in a 200 μL reaction mixture at 37 °C.[33] All assays were conducted under conditions where the reactions were linear with regard to protein concentration and time.

Bacterial Growth and Culture Conditions. *M. smegmatis* and the *menJ* knockout strain, *M. smegmatis* Δ*MSMEG1132*, were maintained in 7H9 Middlebrook medium as described earlier.[44] Wild type *M. tuberculosis* H37Rv and the *menJ* knockout strain, *M. tuberculosis* H37Δ*Rv0561c*, were maintained in 7H9 Middlebrook supplemented with Tween-80 (0.05% v/v) and 10% ADC. For protein expression and lipid extraction, *M. tuberculosis* H37Δ*Rv0561c* transformed with plasmids expressing MenJ or mutant proteins was grown in 7H9 Middlebrook medium supplemented with glucose (0.2% w/v), Tween-80 (0.05% v/v), and hygromycin B (50 μg/mL) in a shaker incubator maintained at 37 °C to an OD_{600} of ∼0.5. The culture was then induced with acetamide (0.2% w/v), incubated for another 120 h, and harvested at 3000 rpm in a CS-6R centrifuge (Beckman).

SDS-PAGE and Immunoblotting. Equal amounts of transformed bacterial cells were analyzed by SDS-PAGE (12%) for immunoblotting. After protein resolution by SDS-PAGE, proteins were transferred to a Whatman Protran BA83 nitrocellulose membrane, and an immunoblot was developed by using BCIP/NBT tablets. Mouse 6X His antibody was used at a dilution of 1:5000, and monoclonal antibodies of anti-GroEL (CS-44, BEI Resources) were used at a dilution of 1:500. The antimouse IgG (whole molecule) alkaline phosphatase antibody (A5153 Sigma Life Science) was used as a secondary antibody.

Lipid Extraction and Identification. Lipid extraction from *M. smegmatis* Δ*MSMEG1132* and *M. tuberculosis* H37Δ*Rv0561c* transformed with plasmids expressing MenJ or mutant proteins was carried out essentially as described earlier[18,20] using chloroform/methanol (2:1 v/v). The extracted lipids were partially purified on a small silicic acid column. Nonpolar lipids from *M. smegmatis* Δ*MSMEG1132* in chloroform were subjected to HPLC mass spectrometry on a Agilent Technologies 1200 HPLC connected to a Agilent Technologies 6210 TOF-MS. HPLC separation was achieved using a Waters X-Bridge C18 column (3.5 μm, 2.1 × 150 mm^2) and a solvent gradient running from 100% methanol to methanol/isopropanol (1:1 v/v) over 60 min at 0.3 mL min^{-1} and 40 °C. Eluted molecules were subjected to positive ion MS using APPI as the ionization interface. The gas temperature was 350 °C, the vaporizer temperature was 300 °C, and the nebulizer pressure was 45 psi. Lipids extracted from *M. tuberculosis* H37Δ*Rv0561c* transformed with plasmid-expressing MenJ or engineered MenJ were analyzed using an Agilent Technologies 1290 Infinity UPLC connected to an Agilent Technologies G6230 LC−MS−TOF. UPLC separation was achieved using an Acquity UPLC-C18 column (1.7 μm, 2.1 × 150 mm^2) and a solvent gradient running from 100% methanol

https://dx.doi.org/10.1021/acsinfecdis.0c00312
ACS Infect. Dis. 2020, 6, 2661−2671

to methanol/isopropanol (1:1 v/v) over 36 min at 0.4 mL min^{-1} and 40 °C. Eluted molecules were subjected to positive ion MS using mixed (APCI and ESI) as the ionization interface. The gas temperature was 325 °C, the vaporizer temperature was 200 °C, and the nebulizer pressure was 35 psi. The data that were obtained were analyzed using Agilent Mass Hunter Workstation software. In all cases, samples were spiked with a known amount of vitamin K2 (MK-4) as an internal standard, and peak area was used to quantitate.[47]

Tissue Culture Conditions. The mouse macrophage-like cell line J774A.1 (ATCC) was cultured at 37 °C in 5% CO_2 in RPMI 1640 medium supplemented with 10% heat-inactivated fetal bovine serum, referred to as complete RPMI medium. The cell density in each culture was monitored using the Cellometer Mini (Nexcelom Bioscience). The viability of cells was monitored by using 0.4% trypan blue.

***In Vitro* Virulence Assessment of MenJ and Mutants.** J774A.1 cells were infected using a multiplicity of infection (MOI) of 5:1 (bacteria/macrophage); J774A.1 cells were incubated with *M. tuberculosis* (H37Rv), *M. tuberculosis* H37Δ*Rv0561c/pMyNT*, *M. tuberculosis* H37Δ*Rv0561c/menj*, *M. tuberculosis* H37Δ*Rv0561c/menj(C46S)*, *M. tuberculosis* H37Δ*Rv0561c/menj(W215L)*, and *M. tuberculosis* H37Δ*Rv0561c/menj(Y213L)*. In all cases, bacterial cultures were treated with 0.2% acetamide prior to infection to induce MenJ expression, and *M. tuberculosis* strains were pelleted by centrifugation at 2000*g*. Bacterial pellets were washed twice in RPMI-1640 media, sonicated in a water bath sonicator for 30 s at room temperature, and passed through a 26-gauge needle 10 times to disrupt any remaining bacterial clumps. Washed bacteria were resuspended in PBS to a final concentration of 1×10^8 cells mL^{-1}. J774A.1 cells were scraped from a T75 cm^2 flask, counted, and infected. Phagocytosis was allowed to proceed for 2 h at 37 °C in a humidified atmosphere containing 5% CO_2. After phagocytosis, the infected cells were washed four times with PBS. To determine the intracellular rate of infection, 1×10^5 cells infected with various strains of *M. tuberculosis* were fixed with 4% paraformaldehyde-PBS overnight and concentrated on slides by centrifugation using a Shandon Cytospin-3 centrifuge. Slides were stained, as previously reported,[48] for acid-fast bacilli using SYBR Gold stain. The dye was diluted 1:1000 in a stain solution consisting of phenol crystals (8 g), glycerin (60 mL), isopropanol (14 mL), and distilled water (26 mL). The slides were flooded with staining solution, warmed on a heating block at 65 °C for 5 min, and then allowed to cool for 3 min at room temperature. Thereafter, the slides were washed in acid alcohol (0.5% HCL, 70% isopropanol) three times at 5 min intervals, washed with water, counterstained with DAPI, and mounted with Prolong Gold Antifade mounting media. Slides were analyzed using a Zeiss LSM 510 confocal microscope equipped with the Zen 2009 software (Zeiss). For *M. tuberculosis* intracellular survival studies, infected macrophages were harvested at the indicated time points and lysed in a bullet blender (Next Advance). Briefly, ~5×10^5 cells/mL were placed in a 1.5 mL sterile safe lock Eppendorf tube containing 0.5 mL of sterile saline. Sterile zirconium oxide beads were added to fill the tube. Cells were homogenized in the bullet blender at 800 rpm for 5 min. The cell homogenate that was obtained was used to enumerate the bacterial load using serial dilutions and plated on 7H11 agar medium supplemented with OADC and hygromycin (50 μg/mL, except in the case of homogenate containing *M. tuberculosis* H37Rv). The plates were incubated at 37 °C for 3 weeks until colonies could be counted.

■ ASSOCIATED CONTENT

Supporting Information

The Supporting Information is available free of charge at https://pubs.acs.org/doi/10.1021/acsinfecdis.0c00312.

Additional methods; a multiple sequence alignment of MenJ proteins and known geranylgeranyl reductases; LC−MS analysis of the lipids isolated from *Mycobacterium smegmatis* Δ*MSMEG1132* transformed with empty plasmid, plasmids encoding MenJ, and MenJ containing point mutations C46S, Y213L, W215L, F217L, and E301G; circular dichroism of Ni-NTA purified wild type MenJ and MenJ containing point mutations C46S, W215L, Y213L, F217L, and E301G; structures and calculated monoisotopic masses of lipoquinones described in this study; lists of bacterial strains; plasmids and primers used in this study; and details of the statistical analysis used (PDF)

■ AUTHOR INFORMATION

Corresponding Author

Dean C. Crick − *Department of Microbiology, Immunology and Pathology, Colorado State University, Fort Collins, Colorado 80523, United States;* orcid.org/0000-0001-9281-7058; Phone: (+1) 970 491 3308; Email: Dean.Crick@colostate.edu; Fax: (+1) 970 491 1815

Authors

Santosh Kumar − *Department of Microbiology, Immunology and Pathology, Colorado State University, Fort Collins, Colorado 80523, United States*

Jordan T. Koehn − *Chemistry Department, Colorado State University, Fort Collins, Colorado 80523, United States;* orcid.org/0000-0003-3008-6303

Mercedes Gonzalez-Juarrero − *Department of Microbiology, Immunology and Pathology, Colorado State University, Fort Collins, Colorado 80523, United States*

Debbie C. Crans − *Chemistry Department, Colorado State University, Fort Collins, Colorado 80523, United States;* orcid.org/0000-0001-7792-3450

Complete contact information is available at: https://pubs.acs.org/10.1021/acsinfecdis.0c00312

Notes

The authors declare no competing financial interest.

■ ACKNOWLEDGMENTS

This research was funded by NIH/NIAID grants AI049151 and AI119567 to D. C. Crick and NSF grant CHE-1709564 to D. C. Crans and D. C. Crick.

■ REFERENCES

(1) Berney, M., and Cook, G. M. (2010) Unique flexibility in energy metabolism allows mycobacteria to combat starvation and hypoxia. *PLoS One 5* (1), No. e8614.

(2) Zhang, Y., Yew, W. W., and Barer, M. R. (2012) Targeting persisters for tuberculosis control. *Antimicrob. Agents Chemother. 56* (5), 2223−2230.

(3) Collins, M. D., and Jones, D. (1981) Distribution of isoprenoid quinone structural types in bacteria and their taxonomic implication. *Microbiol. Rev. 45* (2), 316−354.

(4) Tindall, B. J., Rossello-Mora, R., Busse, H. J., Ludwig, W., and Kampfer, P. (2010) Notes on the characterization of prokaryote strains for taxonomic purposes. *Int. J. Syst. Evol. Microbiol. 60* (Pt 1), 249−266.
(5) Azerad, R., Cyrot, M. O., and Lederer, E. (1967) Structure of the dihydromenaquinone-9 of *Mycobacterium phlei*. *Biochem. Biophys. Res. Commun. 27* (2), 249−252.
(6) Azerad, R., and Cyrot-Pelletier, M. O. (1973) Structure and configuration of the polyprenoid side chain of dihydromenaquinones from Myco- and Corynebacteria. *Biochimie 55* (5), 591−603.
(7) Dunphy, P. J., Gutnick, D. L., Phillips, P. G., and Brodie, A. F. (1968) A new natural naphthoquinone in *Mycobacterium phlei*. Cis-dihydromenaquinone-9, structure and function. *J. Biol. Chem. 243* (2), 398−407.
(8) Holsclaw, C. M., Sogi, K. M., Gilmore, S. A., Schelle, M. W., Leavell, M. D., Bertozzi, C. R., and Leary, J. A. (2008) Structural characterization of a novel sulfated menaquinone produced by stf3 from *Mycobacterium tuberculosis*. *ACS Chem. Biol. 3* (10), 619−624.
(9) Gale, P. H., Arison, B. H., Trenner, N. R., Page, A. C., Jr., and Folkers, K. (1963) Characterization of vitamin K9(H) from *Mycobacterium phlei*. *Biochemistry 2*, 200−203.
(10) Sassetti, C. M., and Rubin, E. J. (2003) Genetic requirements for mycobacterial survival during infection. *Proc. Natl. Acad. Sci. U. S. A. 100* (22), 12989−12994.
(11) Bentley, R., and Meganathan, R. (1982) Biosynthesis of vitamin K (menaquinone) in bacteria. *Microbiol. Rev. 46* (3), 241−280.
(12) Chen, M., Ma, X., Chen, X., Jiang, M., Song, H., and Guo, Z. (2013) Identification of a hotdog fold thioesterase involved in the biosynthesis of menaquinone in *Escherichia coli*. *J. Bacteriol. 195* (12), 2768−2775.
(13) Meganathan, R. (2001) Biosynthesis of menaquinone (vitamin K2) and ubiquinone (coenzyme Q): a perspective on enzymatic mechanisms. *Vitam. Horm. 61*, 173−218.
(14) Sassetti, C. M., Boyd, D. H., and Rubin, E. J. (2003) Genes required for mycobacterial growth defined by high density mutagenesis. *Mol. Microbiol. 48* (1), 77−84.
(15) Griffin, J. E., Gawronski, J. D., Dejesus, M. A., Ioerger, T. R., Akerley, B. J., and Sassetti, C. M. (2011) High-resolution phenotypic profiling defines genes essential for mycobacterial growth and cholesterol catabolism. *PLoS Pathog. 7* (9), No. e1002251.
(16) Li, X., Liu, N., Zhang, H., Knudson, S. E., Slayden, R. A., and Tonge, P. J. (2010) Synthesis and SAR studies of 1,4-benzoxazine MenB inhibitors: novel antibacterial agents against *Mycobacterium tuberculosis*. *Bioorg. Med. Chem. Lett. 20* (21), 6306−6309.
(17) Cook, G. M., Hards, K., Dunn, E., Heikal, A., Nakatani, Y., Greening, C., Crick, D. C., Fontes, F. L., Pethe, K., Hasenoehrl, E., and Berney, M. (2017) Oxidative Phosphorylation as a Target Space for Tuberculosis: Success, Caution, and Future Directions. *Microbiol. Spectrum 5*(3), DOI: 10.1128/microbiolspec.TBTB2-0014-2016.
(18) Dhiman, R. K., Mahapatra, S., Slayden, R. A., Boyne, M. E., Lenaerts, A., Hinshaw, J. C., Angala, S. K., Chatterjee, D., Biswas, K., Narayanasamy, P., Kurosu, M., and Crick, D. C. (2009) Menaquinone synthesis is critical for maintaining mycobacterial viability during exponential growth and recovery from non-replicating persistence. *Mol. Microbiol. 72* (1), 85−97.
(19) Puffal, J., Mayfield, J. A., Moody, D. B., and Morita, Y. S. (2018) Demethylmenaquinone Methyl Transferase Is a Membrane Domain-Associated Protein Essential for Menaquinone Homeostasis in *Mycobacterium smegmatis*. *Front. Microbiol. 9*, 3145.
(20) Upadhyay, A., Fontes, F. L., Gonzalez-Juarrero, M., McNeil, M. R., Crans, D. C., Jackson, M., and Crick, D. C. (2015) Partial Saturation of Menaquinone in *Mycobacterium tuberculosis*: Function and Essentiality of a Novel Reductase, MenJ. *ACS Cent. Sci. 1* (6), 292−302.
(21) Keller, Y., Bouvier, F., D'Harlingue, A., and Camara, B. (1998) Metabolic compartmentation of plastid prenyllipid biosynthesis–evidence for the involvement of a multifunctional geranylgeranyl reductase. *Eur. J. Biochem. 251* (1−2), 413−417.
(22) Hemmi, H., Takahashi, Y., Shibuya, K., Nakayama, T., and Nishino, T. (2005) Menaquinone-specific prenyl reductase from the hyperthermophilic archaeon *Archaeoglobus fulgidus*. *J. Bacteriol. 187* (6), 1937−1944.
(23) Addlesee, H. A., and Hunter, C. N. (2002) *Rhodospirillum rubrum* possesses a variant of the *bchP* gene, encoding geranylgeranyl-bacteriopheophytin reductase. *J. Bacteriol. 184* (6), 1578−1586.
(24) Xu, Q., Eguchi, T., Mathews, I. I., Rife, C. L., Chiu, H. J., Farr, C. L., Feuerhelm, J., Jaroszewski, L., Klock, H. E., Knuth, M. W., Miller, M. D., Dana, W., Elsliger, M. A., Ashley, M. D., Godzik, A., Lesley, S. A., and Wilson, I. A. (2010) Insights into substrate specificity of geranylgeranyl reductases revealed by the structure of digeranylgeranylglycerophospholipid reductase, an essential enzyme in the biosynthesis of archaeal membrane lipids. *J. Mol. Biol. 404* (3), 403−417.
(25) Sasaki, D., Fujihashi, M., Iwata, Y., Murakami, M., Yoshimura, T., Hemmi, H., and Miki, K. (2011) Structure and mutation analysis of archaeal geranylgeranyl reductase. *J. Mol. Biol. 409* (4), 543−557.
(26) Wierenga, R. K., Drenth, J., and Schulz, G. E. (1983) Comparison of the three-dimensional protein and nucleotide structure of the FAD-binding domain of p-hydroxybenzoate hydroxylase with the FAD- as well as NADPH-binding domains of glutathione reductase. *J. Mol. Biol. 167* (3), 725−739.
(27) Dym, O., and Eisenberg, D. (2001) Sequence-structure analysis of FAD-containing proteins. *Protein Sci. 10* (9), 1712−1728.
(28) Meadows, C. W., Mingardon, F., Garabedian, B. M., Baidoo, E. E. K., Benites, V. T., Rodrigues, A. V., Abourjeily, R., Chanal, A., and Lee, T. S. (2018) Discovery of novel geranylgeranyl reductases and characterization of their substrate promiscuity. *Biotechnol. Biofuels 11* (1), 340.
(29) Nishimura, Y., and Eguchi, T. (2007) Stereochemistry of reduction in digeranylgeranylglycerophospholipid reductase involved in the biosynthesis of archaeal membrane lipids from *Thermoplasma acidophilum*. *Bioorg. Chem. 35* (3), 276−283.
(30) Sato, S., Murakami, M., Yoshimura, T., and Hemmi, H. (2008) Specific partial reduction of geranylgeranyl diphosphate by an enzyme from the thermoacidophilic archaeon *Sulfolobus acidocaldarius* yields a reactive prenyl donor, not a dead-end product. *J. Bacteriol. 190* (11), 3923−3929.
(31) Ogawa, T., Isobe, K., Mori, T., Asakawa, S., Yoshimura, T., and Hemmi, H. (2014) A novel geranylgeranyl reductase from the methanogenic archaeon *Methanosarcina acetivorans* displays unique regiospecificity. *FEBS J. 281* (14), 3165−3176.
(32) Kung, Y., McAndrew, R. P., Xie, X., Liu, C. C., Pereira, J. H., Adams, P. D., and Keasling, J. D. (2014) Constructing tailored isoprenoid products by structure-guided modification of geranylgeranyl reductase. *Structure 22* (7), 1028−1036.
(33) Upadhyay, A., Kumar, S., Rooker, S. A., Koehn, J. T., Crans, D. C., McNeil, M. R., Lott, J. S., and Crick, D. C. (2018) Mycobacterial MenJ: An Oxidoreductase Involved in Menaquinone Biosynthesis. *ACS Chem. Biol. 13* (9), 2498−2507.
(34) Rothery, R. A., Chatterjee, I., Kiema, G., McDermott, M. T., and Weiner, J. H. (1998) Hydroxylated naphthoquinones as substrates for *Escherichia coli* anaerobic reductases. *Biochem. J. 332* (Pt1), 35−41.
(35) Jeffery, C. J. (2018) Protein moonlighting: what is it, and why is it important? *Philos. Trans. R. Soc., B 373* (1738).20160523
(36) Henderson, B., and Martin, A. (2011) Bacterial virulence in the moonlight: multitasking bacterial moonlighting proteins are virulence determinants in infectious disease. *Infect. Immun. 79* (9), 3476−3491.
(37) Jeffery, C. J. (2014) An introduction to protein moonlighting. *Biochem. Soc. Trans. 42* (6), 1679−1683.
(38) Kainulainen, V., and Korhonen, T. K. (2014) Dancing to another tune-adhesive moonlighting proteins in bacteria. *Biology (Basel, Switz.) 3* (1), 178−204.
(39) Jeffery, C. J. (2019) Multitalented actors inside and outside the cell: recent discoveries add to the number of moonlighting proteins. *Biochem. Soc. Trans. 47* (6), 1941−1948.

(40) Ingerson-Mahar, M., Briegel, A., Werner, J. N., Jensen, G. J., and Gitai, Z. (2010) The metabolic enzyme CTP synthase forms cytoskeletal filaments. *Nat. Cell Biol. 12* (8), 739−746.
(41) Rao, P. V., Krishna, C. M., and Zigler, J. S., Jr. (1992) Identification and characterization of the enzymatic activity of zeta-Crystallin from guinea pig lens. A novel NADPH:quinone oxidoreductase. *J. Biol. Chem. 267* (1), 96−102.
(42) Rengarajan, J., Bloom, B. R., and Rubin, E. J. (2005) Genome-wide requirements for *Mycobacterium tuberculosis* adaptation and survival in macrophages. *Proc. Natl. Acad. Sci. U. S. A. 102* (23), 8327−8332.
(43) Koehn, J. T., Beuning, C. N., Peters, B. J., Dellinger, S. K., Van Cleave, C., Crick, D. C., and Crans, D. C. (2019) Investigating Substrate Analogues for Mycobacterial MenJ: Truncated and Partially Saturated Menaquinones. *Biochemistry 58* (12), 1596−1615.
(44) Noens, E. E., Williams, C., Anandhakrishnan, M., Poulsen, C., Ehebauer, M. T., and Wilmanns, M. (2011) Improved mycobacterial protein production using a *Mycobacterium smegmatis* groEL1DeltaC expression strain. *BMC Biotechnol. 11*, 27.
(45) Yano, T., Li, L. S., Weinstein, E., Teh, J. S., and Rubin, H. (2006) Steady-state kinetics and inhibitory action of antitubercular phenothiazines on *mycobacterium tuberculosis* type-II NADH-menaquinone oxidoreductase (NDH-2). *J. Biol. Chem. 281* (17), 11456−11463.
(46) Weinstein, E. A., Yano, T., Li, L. S., Avarbock, D., Avarbock, A., Helm, D., McColm, A. A., Duncan, K., Lonsdale, J. T., and Rubin, H. (2005) Inhibitors of type II NADH:menaquinone oxidoreductase represent a class of antitubercular drugs. *Proc. Natl. Acad. Sci. U. S. A. 102* (12), 4548−4553.
(47) Wasinger, V. C., Zeng, M., and Yau, Y. (2013) Current status and advances in quantitative proteomic mass spectrometry. *Int. J. Proteomics 2013*, 180605.
(48) Ryan, G. J., Hoff, D. R., Driver, E. R., Voskuil, M. I., Gonzalez-Juarrero, M., Basaraba, R. J., Crick, D. C., Spencer, J. S., and Lenaerts, A. J. (2010) Multiple *M. tuberculosis* phenotypes in mouse and guinea pig lung tissue revealed by a dual-staining approach. *PLoS One 5* (6), No. e11108.

https://dx.doi.org/10.1021/acsinfecdis.0c00312
ACS Infect. Dis. 2020, 6, 2661−2671